A Max-Min Principle for Phyllotactic Patterns

Wai-Ki Ching, Yang Cong, and Nam-Kiu Tsing

Advanced Modeling and Applied Computing Laboratory,
Department of Mathematics,
The University of Hong Kong, Hong Kong
{wching,congyang}@hkusua.hku.hk, nktsing@hku.hk

Abstract. An interesting phenomenon about phyllotaxis is the divergence angle between two consecutive primordia. In this paper, we consider a dynamic model based on Max-Min principle for generating 2D phyllotactic patterns studied in [2,5]. Under the hypothesis that the influence of the two predecessors is enough to fix the birth place of the new generated primordium, analysis and numerical experiments are conducted. We then propose a new measurement for evaluating the pattern uniformity (sparsity) of different divergence angles. It is found that the golden angle gives very good sparsity but there are other angles give even better sparsity under our proposed measurement.

Keywords: Divergence Angle, Golden Angle, Max-Min Principle, Phyllotactic Patterns.

1 Introduction

The study of geometric and numerical patterns in plants is known as "phyllotaxis". It is a central subject in plant morphogenesis which deals with the arrangements of plant organs such as leaves, bracts, branches, petals, florets, scales, etc. One can see phyllotactic patterns macroscopically when viewing shoot tips. A basic hypothesis is that these phyllotactic patterns result from the conditions of appearance of the primordia near the tip of the growing shoots. The general arrangement of these features is laid down right at the start, as the primordia form [6,8]. The center of the tip is occupied by a stable circular region, which is called "apex". Around the apex, one by one, tiny lumps called "primordia". Each primordium migrates away from the apex which new ones continue to be formed. Eventually, the lump develops into a leaf, petal etc.

The arrangement of sunflower seeds is a common phenomenon. The seeds occur in two families of spirals-one winding clockwise, the other counterclockwise, and appearing to fit through each other. The numbers of the clockwise and counterclockwise spirals are two successive numbers in Fibonacci sequence. Divergence angle, the angles between successive primordia, as seen from the center of the apex, called as divergence angle, are pretty equal, and usually very close to 137.5°. The most efficient packing, the one that makes the most solid and robust seed head, occurs when the divergence angle is equal to the golden angle, 137.5° [9].

Douady and Couder [3] used a physical analogue to implement a laboratory experiment: A circular dish filled with silicone oil and placed in a magnetic field. Let tiny drops of magnetic fluid fall at regular intervals into the center of the dish. The drops were polarized by the magnetic field, and they repelled each other; they were given a boost in the radial direction by making the magnetic field stronger at the edge of the dish than it was in the middle. The patterns that appeared depends on how big the intervals between drops were. A very prevalent pattern was the one in which successive drops lay on a spiral with a divergence angle very close to $137.5°$, the golden angle, giving a sunflower seed pattern of interlaced spirals-one winding clockwise and the other counterclockwise whose numbers are two consecutive numbers in the Fibonacci series.

Douady and Couder [3] assume that the elements repel each other, like equal electrical charges or magnets with the same polarity. This repulsion ensures that the outward motion keeps going, and that each new primordia appears as far as possible from its immediate predecessors [3]. It was suggested that a new primordium appears with a periodicity T near the tip in the largest gap left between the previous primordia and the apex [4]. Under this assumption, Atela, Golé and Hotton provided a Max-Min dynamical model to study 3D pattern formation [2]. They choose the point on the apex circle where the minimum distance with all existing primordia is the maximum as the birth place of the new primordium. Furthermore, they suggest that one only needs to consider some primordia "before" the new born one instead all primordia. Later, they study 2D pattern formation problem under Max-Min principle, where they consider the influence of all existing primordia [5].

Inspired by the early work in [3] and the dynamical system model [2,5], we implement the Max-Min principle to discuss 2D phyllotaxis problem. The model in our study only considers the interaction between the new born primordium with its two predecessors.

The remainder of this paper is structured as follows. In Section 2, we present our Max-Min model. In Section 3, we provide a measure to evaluate the uniformity of patterns and some numerical results. Finally, concluding remarks are given in Section 4 to address further research issues.

2   The Max-Min Principle

In this section, we present the mathematical model based on the Max-Min principle for the development of 2D phyllotactic patterns. The followings are the assumptions of the model based on the proposed Max-Min principle [2,5].

(i) The stem apex is axisymmetric represented by a circle of given radius R_0 from a center in a plane surface;

(ii) Identical primordia are generated with a periodicity T at the periphery of the apex;

(iii) Due to the shoot's growth, primordia move away from the center. Here we assume that the area of the circle between the primordium and the origin

grows at a constant speed, the distance between the primordia and the circle equals to

$$R_0 + V\sqrt{t}.$$

In fact, one can also consider $R_0 + Vt^s$ where $0 < s$ (say $s = 1$) to obtain similar results.

(iv) Outside of the region of radius R_0, there is no further reorganization leading to changes of the angular positions of the primordia.

To facilitate our discussion, we label the primordia according to their emergence sequence. We define θ_i to be the angle between the straight line joining the origin and the ith primordium and the positive x axis. Then at the emergence of the kth primordia $(k > i)$, the coordinate of the ith primordia is given by

$$((R_0 + V\sqrt{k-i})\cos\theta_i, (R_0 + V\sqrt{k-i})\sin\theta_i).$$

To decide the position of the birth of a new primordia on the disc of radius R_0 (suppose the kth one), one only needs to find the angle θ_k. We assume that for a given point around the periphery of the apex $(R_0\sin\theta, R_0\cos\theta)$, we use the usual Euclidean distance:

$$E(d_i) = \sqrt{\left((R_0 + V\sqrt{k-i})\cos\theta_i - R_0\cos\theta\right)^2 + \left((R_0 + V\sqrt{k-i})\sin\theta_i - R_0\sin\theta\right)^2}$$

$$(1)$$

to measure the influence of the ith primordium to this point. We adopt the Max-Min principle [2,5]: to minimize the influence of other primordia is to maximize the minimum distances with other primordia. We then define the following objective function for our model:

$$\theta_k = \max_{0 \le \theta < 2\pi} \left\{ \min_{i \in \{1,2,\dots,k-1\}} \{E(d_i)\} \right\}. \tag{2}$$

Here we hypothesize that only the $(k-1)$th and the $(k-2)$th primordia make contribution to determine the birth place of the kth primordium. Thus Definition (2) can be simplified as follows (this makes the problem mathematically tractable) :

$$\max_{0 \le \theta < 2\pi} \left\{ \min_{i=k-1,k-2} \{E(d_i)\} \right\}. \tag{3}$$

It is straightforward to check that θ_k, the optimal angle of (3), satisfies the the following equality:

$$E(d_{k-1}) = E(d_{k-2}). \tag{4}$$

This yields

$$V^2 + 2(\sqrt{2}-1)R_0V + 2R_0(R_0+V)\cos(\theta_k - \theta_{k-1}) - 2R_0(R_0 + \sqrt{2}V)\cos(\theta_k - \theta_{k-2}) = 0.$$

$$(5)$$

Actually in the numerical experiments, $\theta_k - \theta_{k-1}$ converges to an angle α. By (5), $\cos(\alpha)$ satisfies

$$4R_0(R_0+\sqrt{2}V)\cos^2\alpha - 2R_0(R_0+V)\cos\alpha - (2R_0^2+(4\sqrt{2}-2)R_0V+V^2) = 0 \quad (6)$$

or equivalently

$$4(1+\sqrt{2}\tau)\cos^2\alpha - 2(1+\tau)\cos\alpha - (2+(4\sqrt{2}-2)\tau+\tau^2) = 0 \quad (7)$$

where $\tau = V/R_0$. In fact, there is one-to-one relation between τ and α, see for instance the proof in Appendix. If τ is given, it can be shown that there exists a unique α satisfying

$$\cos\alpha = \frac{(1+\tau) - \sqrt{(1+\tau)^2 + 4(1+\sqrt{2}\tau)(2+(4\sqrt{2}-2)\tau+\tau^2)}}{4(1+\sqrt{2}\tau)}. \quad (8)$$

On the other hand, if α is given, it can be shown that there exists a unique τ satisfying

$$\tau = -(1-\cos\alpha)(2\sqrt{2}(1+\cos\alpha)-1)$$
$$+\sqrt{(1-\cos\alpha)^2(2\sqrt{2}(1+\cos\alpha)-1)^2 - 2(1-\cos\alpha)(1+2\cos\alpha)}.$$

The golden pair is $(\tau, \theta) = (1.8058, 137.5°)$.

Figure 1 reports the phyllotaxis generated under the following parameters

$$n = 600, \quad V = 1.8058, \quad R_0 = 1 \quad (9)$$

where n is the number of primordium. Almost all the divergence angles of the simulated packing are equal to $137.5°$, which is golden angle. In the rest of this paper, without special announcement, numerical experiments are all done under the parameter pair $n = 600, R_0 = 1$.
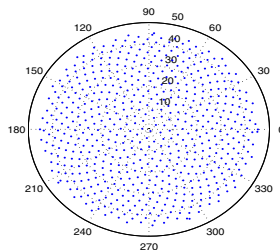

Fig. 1. The packing pattern with the golden divergence angle

3 Uniformity of Packing and Simulation Results

3.1 Uniformity of Packing

From the simulation results, there are some divergence angles which can form packing patterns similar to sunflower. To measure the uniformity of packing, we define the following indicator. Under different velocity v, the area that the corresponding pattern covers varies. Thus to make a fair uniformity (sparsity) measurement, we firstly map the packing pattern into a disk with radius equals to one. We then define the uniformity measurement as the sum of the minimum distance of each node with others

$$I(n, V, R) = \frac{1}{n} \sum_{i=1}^{n} \min_{j} d(i, j). \tag{10}$$

where $d(i, j)$ is the distance between the ith and jth primordium, then divide this sum by n the number of primordia. It is obvious that the bigger the value is, the more even (sparse) the packing is.

3.2 Simulation Results

Figure 2 illustrates the relationship between the velocity V and the uniformity $I(n, V, R)$ of the corresponding pattern. There are many local maximum points and local minimum points.

Figure 3 shows packing patterns with corresponding divergence angles, generated by V corresponding to several local minimum points respectively. Under the velocity V of these local minimum points, the patterns generated are not uniformly sparse. On the other hand, we illustrate the patterns generated by V corresponding to those local maximum points respectively in Figure 4. These
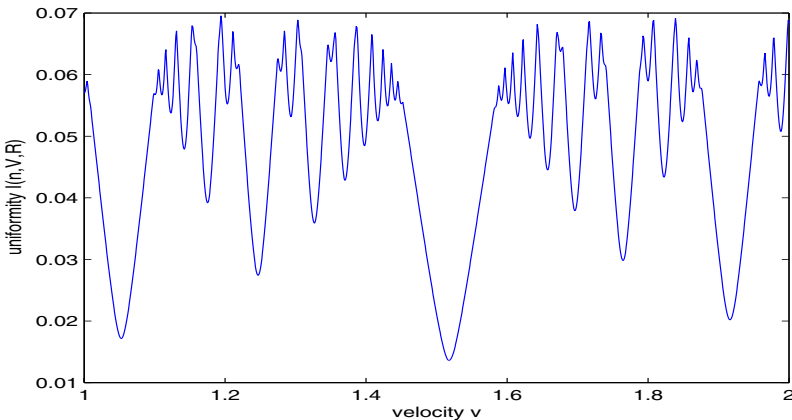

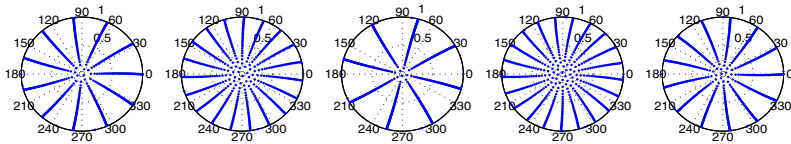**Fig. 2.** Relationship between v and pattern uniformity $I(n, V, R)$

Fig. 3. (a)$V = 1.053, \alpha = 130.91°$ (b)$V = 1.247, \alpha = 132.63°$ (c)$V = 1.518, \alpha = 135.00°$ (d)$V = 1.765, \alpha = 137.15°$ (e)$V = 1.916, \alpha = 138.46°$
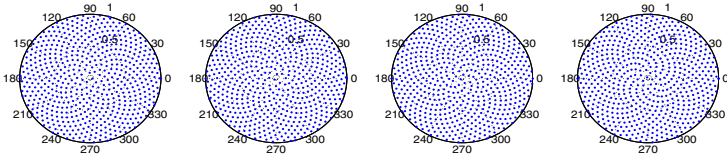

Fig. 4. (a)$V = 1.194, \alpha = 132.17°$ (b)$V = 1.303, \alpha = 133.13°$ (c)$V = 1.717, \alpha = 136.73°$ (d)$V = 1.839, \alpha = 137.79°$

Table 1. Comparison among pattern information generated by V of some local maximum points

	$V = 1.8058$	$V = 1.194$	$V = 1.303$	$V = 1.717$	$V = 1.839$
The divergence angle	$137.50°$	$132.17°$	$133.13°$	$136.73°$	$137.52°$
$I(n, V, R)$	0.06669	0.06951	0.06883	0.06863	0.06914

patterns are uniform and similar to the pattern with divergence angle $137.5°$. We note that $V = 1.8058$ which generates the golden angle pattern is among the x-coordinates of local maximum points in Figure 2.

Table 1 shows the comparison among velocity, divergence angle and uniformity of their corresponding patterns shown in Figures 2 and 4. We find that there exist some sparse patterns with higher uniformity (sparsity) than the pattern with the golden angle.

3.3   Conclude Remarks

In this paper, we implement the Max-Min principle [2,5] to determine the place of birth of a new primordia in a 2D setting. There are some questions remain open. First we expect to extend the model to a 3D setting. Second under our new measurement of uniformity, there are other angles different from the golden angle which perform very well. We are looking forward to examining the reasons. Furthermore, we will further explore the Min-Distance Principle approach for patterns under low uniformity.

References

1. Adler, I.: A model of space filling in phyllotaxis. J. Theoret. Biol. 53(2), 435–444 (1975)
2. Atela, P., Golé, C., Hotton, S.: A Dynamical System for Plant Pattern Formation: Rigorous Analysis. J. Nonlinear Sci. 12(6), 641–676 (2002)
3. Douady, S., Couder, Y.: Phyllotaxis as a physical self-organized growth process. Phys. Rev. Lett. 68, 2098–2101 (1992)
4. Hofmeister, W.: Allgemeine Morphologie der Gewachse, Handbuch der Physiologishen Botanik, pp. 405–664. l Engelman, Leipzig (1868)
5. Hotton, S., Johnson, V., Wilbarger, J., Zwieniecki, K., Atela, P., Golé, C., Dumais, J.: The Possible and the Actual in Phyllotaxis: Bridging the Gap between Empirical Observations and Iterative Models. J. Plant Growth Regul. 25, 313–323 (2006)
6. Jean, R.V.: Mathematical Approach to Patterns and Form in Plant Growth. Wiley, New York (1984)
7. Marzec, C., Kappraff, J.: Properties of maximal spacing on a circle related to phyllotaxis and to the golden mean. J. Theoret. Biol. 103(2), 201–226 (1983)
8. Steeves, R.V., Sussex, I.M.: Patterns in Plant Development. Cambridge University Press, Cambridge (1989)
9. Vogel, H.: A better way to construct the sunflower head. Mathematical biosciences 44, 145–174 (1979)

A   Appendix: The Calculation of θ_k

Since we have $E(d_{k-1}) = E(d_{k-2})$, it yields

$$((R_0 + V)\cos\theta_{k-1} - R_0\cos\theta_k)^2 + ((R_0 + V)\sin\theta_{k-1} - R_0\sin\theta_k)^2 = ((R_0 + \sqrt{2}V)\cos\theta_{k-2} - R_0\cos\theta_k)^2 + ((R_0 + \sqrt{2}V)\sin\theta_{k-2} - R_0\sin\theta_k)^2. \tag{11}$$

We can deduce the value of θ_k by the following steps. By direct verification of the above equation, we have

$$V^2 + 2(\sqrt{2} - 1)R_0V + 2R_0(R_0 + V)(\cos\theta_k\cos\theta_{k-1} + \sin\theta_k\sin\theta_{k-1}) \\ -2R_0(R_0 + \sqrt{2}V)(\cos\theta_k\cos\theta_{k-2} + \sin\theta_k\sin\theta_{k-2}) = 0. \tag{12}$$

Further, we can write the above formula as

$$V^2 + 2(\sqrt{2} - 1)R_0V + 2R_0(R_0 + V)\cos(\theta_k - \theta_{k-1}) - 2R_0(R_0 + \sqrt{2}V)\cos(\theta_k - \theta_{k-2}) = 0. \tag{13}$$

Assuming α is the angle between θ_k and θ_{k-1}, θ is the angle between θ_{k-1} and θ_{k-2}, then we have

$$V^2 + 2(\sqrt{2} - 1)R_0V + 2R_0(R_0 + V)\cos\alpha - 2R_0(R_0 + \sqrt{2}V)\cos(\theta + \alpha) = 0.$$

We suppose for a uniformed phyllotactic pattern, the angle between each two consecutive primordia tends to a same value. Thus $\alpha = \theta$ holds and we have

$$4R_0(R_0 + \sqrt{2})\cos^2\alpha - 2R_0(R_0 + V)\cos\alpha - (2R_0^2 + (4\sqrt{2} - 2)R_0V + V^2) = 0.$$

Thus we have

$$\cos\alpha = \frac{R_0(R_0 + V) - \sqrt{R_0^2(R_0 + V)^2 + 4R_0(R_0 + \sqrt{2}V)(2R_0^2 + (4\sqrt{2} - 2)R_0V + V^2)}}{4R_0(R_0 + \sqrt{2}V)}$$

(14)

because

$$\frac{R_0(R_0 + V) + \sqrt{R_0^2(R_0 + V)^2 + 4R_0(R_0 + \sqrt{2}V)(2R_0^2 + (4\sqrt{2} - 2)R_0V + V^2)}}{4R_0(R_0 + \sqrt{2}V)} > 1.$$

(15)

This is true because

$$R_0^2(R_0+V)^2+4R_0(R_0+\sqrt{2}V)(2R_0^2+(4\sqrt{2}-2)R_0V+V^2) > \left(4R_0(R_0 + \sqrt{2}V) - R_0(R_0 + V)\right)^2.$$

(16)

The kth primordia fills in the biggest gap which gets the minimum repelling energy by its consecutive two ancestors, the $(k-1)$th and $(k-2)$th. The divergence angle between two consecutive primordia should be bigger than 90° and smaller than 180°. Since

$$\sqrt{R_0^2(R_0 + V)^2 + 4R_0(R_0 + \sqrt{2}V)(2R_0^2 + (4\sqrt{2} - 2)R_0V + V^2)} > R_0(R_0 + V),$$

(17)

we have

$$\cos\alpha = \frac{R_0(R_0 + V) - \sqrt{R_0^2(R_0 + V)^2 + 4R_0(R_0 + \sqrt{2}V)(2R_0^2 + (4\sqrt{2} - 2)R_0V + V^2)}}{4R_0(R_0 + \sqrt{2}V)} < 0.$$

(18)